Unveiling nickelocene bonding to a noble metal surface

N. Bachellier,[1] M. Ormaza,[1] M. Faraggi,[2] B. Verlhac,[1] M. Vérot,[3] T. Le Bahers,[3] M.-L. Bocquet,[2] and L. Limot[1,*]

[1]*IPCMS, CNRS UMR 7504, Université de Strasbourg, 67034 Strasbourg, France*

[2]*Département de Chimie, École Normale Supérieure, ENS-CNRS-UPMC UMR 8640, 75005 Paris, France*

[3]*Université de Lyon, Université Claude Bernard Lyon 1, CNRS, ENS Lyon, 69007 Lyon, France*

(Received 14 February 2016; revised manuscript received 5 April 2016; published 2 May 2016)

The manipulation of a molecular spin state in low-dimensional materials is central to molecular spintronics. The designs of hybrid devices incorporating magnetic metallocenes are very promising in this regard, but are hampered by the lack of data regarding their interaction with a metal. Here, we combine low-temperature scanning tunneling microscopy and density functional theory calculations to investigate a magnetic metallocene at the single-molecule level—nickelocene. We demonstrate that the chemical and electronic structures of nickelocene are preserved upon adsorption on a copper surface. Several bonding configurations to the surface are identified, ranging from the isolated molecule to molecular layers governed by van der Waals interactions.

DOI: 10.1103/PhysRevB.93.195403

I. INTRODUCTION

Spintronics exploits the spin of electrons in addition to their charge to potentially offer electronic devices of greater efficiency. A considerable effort is being devoted at including specifically designed molecules into spintronic devices to explore new functionalities [1]. The manipulation of the molecular spin state via the bonding configuration [2–8], doping [9–12], or magnetic coupling [13] of the molecule can, for example, be used to control spin-related phenomena. The miniaturization of devices also calls for the development of low-dimensional spintronic materials. Metallocenes are extremely appealing in both regards. In their most common version, they are composed by one of the six elements in the middle of the 3*d* row (V, Cr, Mn, Fe, Co, Ni) sandwiched between two cyclopentadienyl rings (C_5H_5, hereafter referred to as Cp; see Fig. 1 for the molecular structure). Since their magnetic moments depend on the nature of the 3*d* transition atom, chains of metallocene molecules—eventually encapsulated into carbon nanotubes [14,15]—can be envisioned with the desired magnetic properties. Some of these chains are even predicted to be half metals and could serve as efficient filters for spin-polarized charge carriers [16–20].

Despite this exciting prospect, the design of hybrid devices incorporating magnetic metallocenes has been held up by the lack of knowledge concerning their interaction with a metal. For instance, nickelocene ($NiCp_2$), which is well representative of magnetic metallocenes [21], has been the subject of only a handful of studies [22–26], none being carried out at the single-molecule level. Important aspects need still to be addressed regarding the stability on metals. The d^8 configuration of nickel results in an electronic structure of $(e_2)^4(a_1)^2(e_1)^2$ for nickelocene (Fig. 1), which endows the molecule with a spin $S = 1$. This open valence shell, however, makes nickelocene chemically more reactive than its nonmagnetic counterpart, i.e., ferrocene ($FeCp_2$), which instead possesses a closed shell of 18 electrons. Upon adsorption, such reactivity can be detrimental to the magnetic moment because of charge transfer towards the surface [27,28] and can even jeopardize the chemical integrity of the molecule on some surfaces [22,23], which would make then the interest for nickelocene rather questionable. Puzzling and contradictory results have also been obtained by macroscopic averaging techniques regarding the assembly of nickelocene molecules on metal surfaces, in particular, on Ag(100). In one study, nickelocene was reported to bond with the molecular axis canted away from the surface normal—possibly with the molecular axis parallel to the surface [22]. In another study [25], two bonding configurations were reported, one with the axis along the surface normal and another one appearing at higher coverages where the axis is canted. The adsorption of nickelocene remains elusive up to now.

All these pressing questions call for an atomic-scale study of the bonding configurations of nickelocene to a metal surface. Here, we focus onto a prototypical system consisting of single nickelocene molecules adsorbed on a Cu(100) surface. Through a combined scanning tunneling microscopy (STM) and density functional theory (DFT) study we demonstrate that the chemical and electronic structures of nickelocene are preserved on the metal. We identify, in particular, the existence of several bonding configurations of nickelocene to the surface spanning from the isolated molecule to stable two-dimensional assemblies governed by van der Waals (vdW) interactions.

The measurements were performed with a STM working in ultrahigh vacuum at 4.4 K (see the Methods section in the Supplemental Material [29] for details). The submonolayer deposition of nickelocene (hereafter referred to as Nc) onto the cold Cu(100) surface (see Methods) gives rise to well-ordered molecular assemblies as shown in Fig. 2(a), but also results in large surface areas covered by isolated molecules [Fig. 2(b)]. Only one molecular species is present on the surface, at variance with photoemission studies reporting some traces of fragmentation [22]. Rather, our findings agree with previous observations reported for the less reactive Ag(100) surface [24,26]. Similar to Ag(100), we also found that subsequent annealing above 230 K results in the appearance of several molecular species, suggesting a decomposition of Nc.

*limot@ipcms.unistra.fr

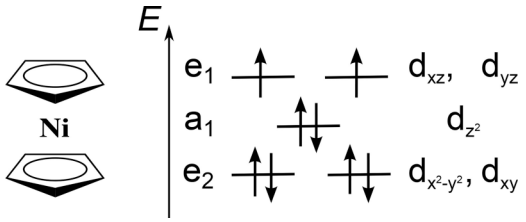

FIG. 1. *d* manifold of gas phase nickelocene in the D_{5h} eclipsed symmetry. The *z* direction is taken along the molecular axis.

The ringlike shape observed in the STM images [Fig. 2(c); see also Fig. 3(a)] indicates that the Nc is bonded to the surface through a Cp ring, while the other Cp ring is exposed to vacuum. In other words, the molecular axis is perpendicular to the surface; hereafter we define these molecules as "vertical" nickelocenes. Isolated and self-assembled molecules have distinct apparent heights of (3.5 ± 0.1) Å and (4.0 ± 0.2) Å relative to Cu(100) [Figs. 2(c) and 2(d)], although Nc molecules at the edge of the molecular assembly [see the arrow in Fig. 2(c)] exhibit an apparent height close to the isolated ones. The different apparent heights highlight changes in the bonding configurations of these molecules to the surface. As we will see later, these differences result from the presence in the layer of Nc molecules with the molecular axis parallel to the surface, which we define as "horizontal" nickelocenes. For clarity, we first focus on the adsorption properties of isolated Nc and then turn to the assembly of nickelocene on copper.

II. ISOLATED NICKELOCENE

Ferrocene (hereafter referred to as Fc) was recently investigated in similar conditions as the present work [30] and was shown to exclusively physisorb on copper surfaces in an assembly governed by vdW interactions. The presence here of isolated molecules then indicates that nickelocene is more reactive to the surface. Supporting this conclusion, we found that isolated Nc is preferentially adsorbed on copper with the bottom Cp ring centered on the hollow site of Cu(100) [Fig. 3(a)]. The adsorption site was determined by enhancing the spatial resolution of the STM through a tip-assisted manipulation of a Cu atom [31,32]. After dosing a small amount of copper atoms onto the cold Cu(100) surface (see Methods), a Cu atom was dragged with the tip to image the corrugation of Cu(100) [the inset of Fig. 3(a)], which is otherwise not observable in normal tunneling conditions due to the compact nature of the surface. The Cu atoms also serve as markers to identify the position of the hollow sites of Cu(100). A grid representing the Cu(100) surface, which is extracted from the manipulated atom image, can then be positioned in Fig. 3(a) so that the copper atoms are located in a hollow position and hence the adsorption site of Nc can then be determined.

To confirm these findings, we implemented DFT calculations on a system composed of an isolated Nc molecule on Cu(100) (see Methods in the Supplemental Material for details). We performed an energetic analysis of the adsorption of nickelocene relaxed in three highly symmetric sites by centering the Cp ring in a top, bridge, and hollow site of Cu(100) [Fig. 3(b)]. From the analysis, which was carried out with

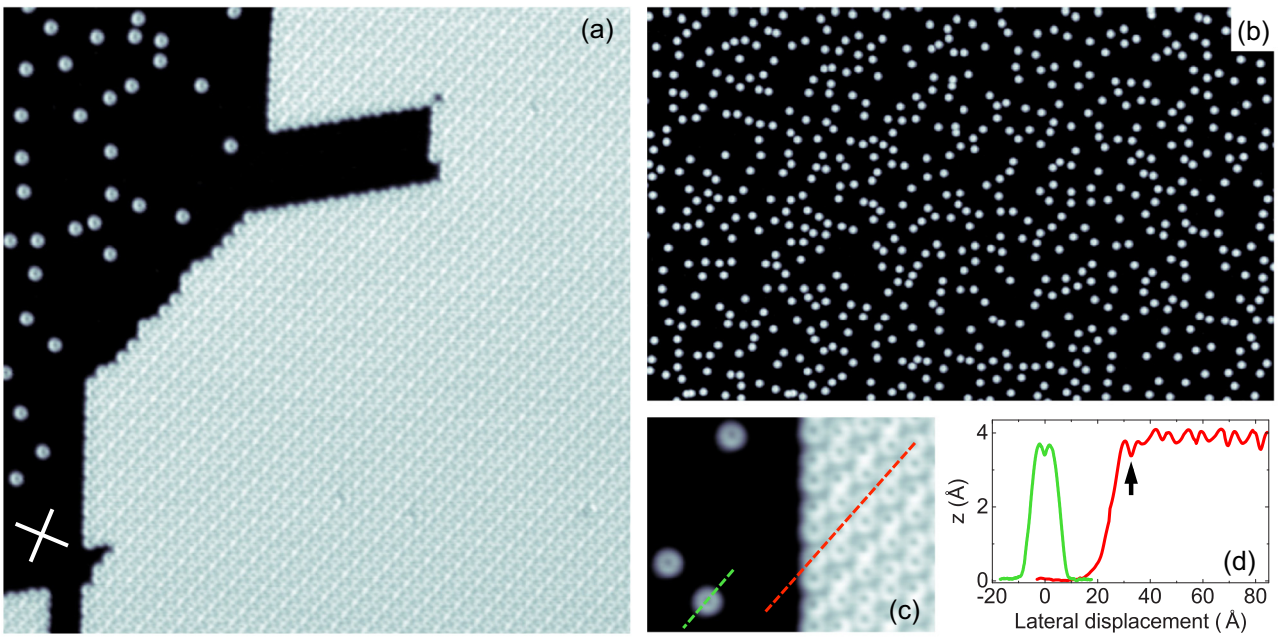

FIG. 2. (a) Self-assembled layer (paired configuration) and isolated Nc on Cu(100) (image size: 500×500 Å^2; sample bias: 20 mV; tunneling current: 50 pA). The cross indicates the crystallographic directions of the Cu(100) surface. (b) Large area with isolated molecules only (650×1000 Å^2, 10 mV, 50 pA). Coverage is 0.045 monolayers. A monolayer is defined relative to the molecular layer, which has a surface density of eight molecules per 260 Å^2 (Table II). (c), (d) Close-up view (75×90 Å^2) at a layer edge, along with (c) the height profiles of the layer and of isolated Nc. The profiles are acquired along the dashed lines indicated in (c). The arrow in (d) highlights a Nc molecule at the edge of the layer.

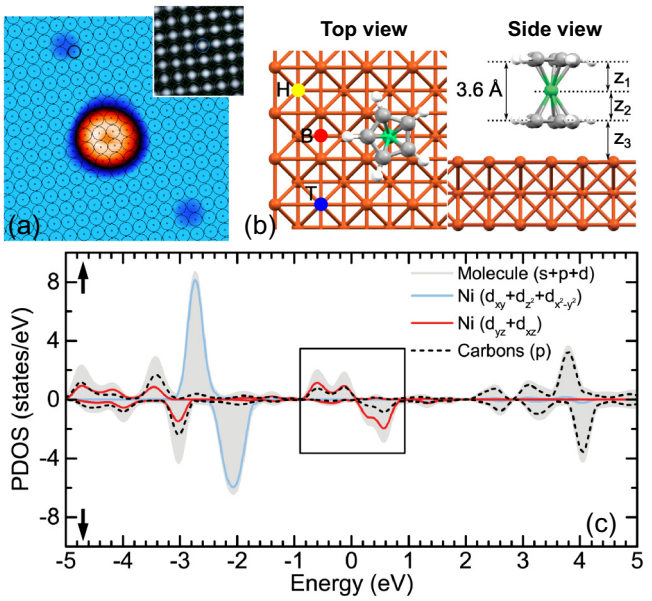

FIG. 3. (a) STM image of isolated Nc (40×40 Å^2, 20 mV, 50 pA) and simulated (100) lattice revealing the adsorption of nickelocene. Two Cu atoms are also visible. Inset: Image of the Cu(100) surface obtained by a tip-assisted manipulation of a Cu atom on a pristine area of the surface (16.5×16.5 Å^2, 10 mV, 80 nA). The copper lattice is 2.52 Å. (b) Top and side view of the structural model of eclipsed Nc on Cu(100) (green: Ni; gray: C; white: H). Top (T), bridge (B), and hollow (H) adsorption sites are depicted in the top view image. (c) Projected density of states (PDOS) of Nc onto different molecular and atomic orbitals (up arrow: majority spins; down arrow: minority spins). The light-gray area corresponds to the entire molecule projected on s, p, and d orbitals. The nickel d orbital is grouped as $d_{yz} + d_{xz}$ (solid red line) and as $d_{xy} + d_{z^2} + d_{x^2-y^2}$ (solid blue line). The dashed black line corresponds to the contribution of all p carbon orbitals. The box between -1 and 1 eV shows the spin-polarized LUMO.

three approaches Perdew-Burke-Ernzerhof (PBE), DFT-D2, and optPBE density functionals [33], we can assess that nickelocene preferentially adsorbs vertically, the horizontal orientation being higher in energy by roughly 400 meV, and that the hollow site corresponds to the most stable adsorption site, in agreement with experiments. We examined both eclipsed (D_{5h} symmetry) and staggered (D_{5d} symmetry) geometries, the latter having the two Cp rings rotated by 36° with respect to each other, and found similar electronic structures. We note, however, that the eclipsed configuration is 23 meV lower in energy for the free molecule and probably favored upon adsorption. The eclipsed nickelocene placed vertically is moderately chemisorbed with an adsorption energy of -0.93 eV within the optPBE functional and -1.33 eV with DFT-D2 (see Table S1 in the Supplemental Material). In the isolated adsorption state the Bader charge analysis [34,35] shows a minor $0.1e$ charge transfer from the molecule to the surface.

The scenario of moderate chemisorption of Nc is also consistent with the bonding distances computed for isolated nickelocene and ferrocene on Cu(100) (Table I). Since the Fc molecule has a closed shell valence configuration of $(e_2)^4(a_1)^2$, it is less prone to interacting with the metal compared to Nc.

TABLE I. Bonding distances z_1, z_2, z_3 of Nc and Fc expressed in Å [see Fig. 3(b)]. The results were obtained with DFT-D2. Columns one and two were calculated with the metallocenes in a hollow site of Cu(100). The higher values of z_1 and z_2 for Nc compared to the Fc result from the antibonding character of the e_{1g} orbitals, which are occupied in nickelocene.

	Nc/Cu(100)	Fc/Cu(100)	Nc (gas phase)
z_1	1.77	1.64	1.79
z_2	1.78	1.62	1.81
z_3	2.35	3.15	

The interaction of Fc is therefore governed by vdW interactions resulting in a larger bond equilibrium distance (noted z_3 in Table I) than nickelocene. The bonding distances within the Nc molecule (noted z_1 and z_2) compare well to those computed (Table I) or measured [36] in the gas phase, indicating that Nc does not deform upon adsorption.

The atomic-orbital projected density of states is plotted in Fig. 3(c). The shaded light-gray area in Fig. 3(c) corresponds to the sum of the s, p, and d orbitals of the entire molecule, whereas the red line groups d_{yz} and d_{xz} and the blue line considers d_{xy}, d_{z^2}, and $d_{x^2-y^2}$. The lowest unoccupied molecular orbital of Nc [LUMO—see the box in Fig. 3(c)] can be qualitatively represented by the mixing of C and Ni contributions placed around the Fermi level and is clearly spin polarized, giving a magnetic character to the molecule. The rest of the Ni($3d$) shell (blue line) is occupied and nonmagnetic. The magnetic moment of Nc amounts to $1.96\mu_B$ ($1.18\ \mu_B$ for the nickel atom) and is practically unchanged compared to the gas phase ($2\mu_B$). Upon adsorption, the magnetic moment of nickelocene is preserved ($S \approx 1$) and the electronic structure corresponds to the schematic picture given for the gas phase molecule in Fig. 1.

III. NICKELOCENE ASSEMBLY

As anticipated in Fig. 2, nickelocene also adsorbs associatively to form well-ordered layers. The molecules self-assemble in two possible molecular configurations equally distributed across the surface, which hereafter we label as "paired" [Fig. 4(a)] and "compact" [Fig. 4(b)]. Four possible orientations relative to the copper surface are evidenced for both configurations with angles $\phi = (53 \pm 3)°, -\phi, (90° + \phi)$, and $(90° - \phi)$ [see ϕ in Figs. 4(a) and 4(b)]. Similar molecular assemblies are observed on Cu(111) (Fig. 5 and Table II) and are therefore independent of the surface symmetry, hinting towards a weak coupling of the layer to the copper surface.

In the paired layer, vertical Nc molecules are arranged following dimerlike pairs with variable Nc-Nc spacing of (7.9 ± 0.3) Å [the solid line in Fig. 4(a)] and of (6.5 ± 0.3) Å [the dashed line in Fig. 4(a)], while the spacing among the dimerlike pairs is (9.0 ± 0.3) Å. The corrugation is at most 0.6 Å [Fig. 4(c)], but some differences are evident among the two type of pairs. In the pairs with smallest Nc-Nc spacing, the ringlike protrusion of the Cp rings has nearly the same corrugation. The molecules are practically vertical and, therefore, in a configuration similar to that of isolated molecules. On the contrary, for larger Nc-Nc spacing, the

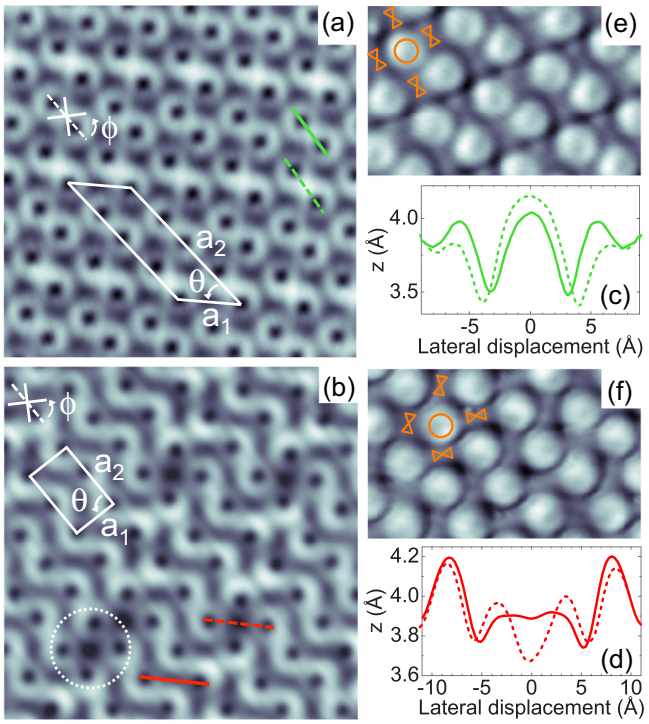

FIG. 4. STM image of the (a) paired and (b) compact layers (70×70 Å^2, 20 mV, 20 pA). The unit cells are shown by solid lines. The layers are tilted by an angle ϕ relative to the crystallographic directions of Cu(100), which are depicted by a cross. The dashed circle in (b) highlights a defect in the compact layer. (c), (d) Height profiles acquired in the paired [green lines in (a)] and compact [red lines in (b)] layers. (e), (f) Images of the paired and compact layers, respectively, acquired with a low tunneling bias (28×46 Å^2, 1 mV, 10 pA). The molecular arrangement is sketched in orange on both images (circle: vertical Nc; hourglass: horizontal Nc).

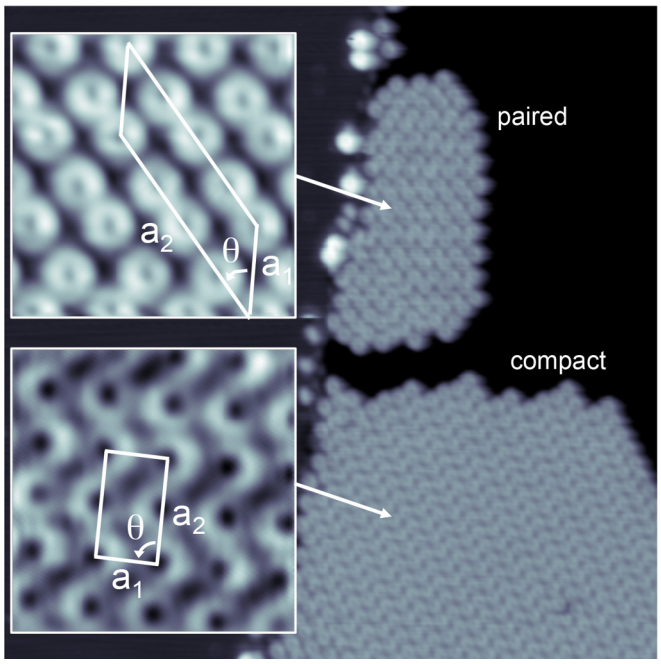

FIG. 5. Nickelocene adsorption on Cu(111) (380×380 Å^2). The close-up views of the two configurations (40×40 Å^2) underline the similarity with the self-assembled layers found for nickelocene on Cu(100). The unit cell parameters for both arrangements (white solid lines) as well as the apparent height of the molecular layers relative to copper (4.2 ± 0.1 Å) are almost identical to the parameters obtained for Cu(100). Images acquired with 20 pA and 0.1 V.

corrugation increases by 0.15 Å in the center of the pair and, concomitantly, decreases by the same amount at the edges of the pair, indicating then that the two molecules are tilted with opposite angles. As the two types of pairs are arranged in alternating rows, the unit cell is a parallelogram with lattice parameters a_1, a_2, and angle θ (Table II), as shown by the solid white line in Fig. 4(a).

The dimerlike pairing of nickelocene recalls that of ferrocene [30], and ferrocene-derived molecules [37,38] on copper surfaces. The intermolecular arrangement is also similar to that encountered for ferrocene where horizontal and vertical molecules are present in the layer. The detection of the horizontal nickelocene is, however, experimentally demanding. To visualize them, we acquired low-bias images to minimize the corrugation of the Cp rings [Fig. 4(e)]. The horizontal molecules are then imaged as elongated rodlike protrusions flanking Nc molecules and aligned in the same direction. There are a total of eight molecules—horizontal and vertical—per unit cell and the packing density is 0.030 molecules/Å^2, which is remarkably close to the packing density of 0.029 molecules/Å^2 of ferrocene on Cu(111) [30].

The compact assembly [Fig. 4(b)] has instead a rectangular unit cell with a maximum corrugation of 0.5 Å [the solid line in Fig. 4(d)]. The unit cell is close to the one encountered for the compact layer of Fc molecules on Cu(111). Along with the similar lattice parameters (Table II), other distinctive features of the Fc compact layer can in fact be recognized. First, the vertical molecules are tilted, as is evident by the corrugation of the imaged Cp ring, center, and corner molecules of the unit cell being tilted in opposite directions. Second, the horizontal molecules, which are again observable via a low-bias image [Fig. 4(f)], flank the Nc molecules, alternating between two possible orientations. There are a total of four molecules in the unit cell and the packing density is again 0.030 molecules/Å^2. The compact assembly of nickelocene, unlike the one of ferrocene, presents defects that are imaged as dim spots in the layer. One defect is highlighted by a dashed circle in Fig. 4(b). Given the 0.2 Å corrugation of a defect [the dashed line in Fig. 4(d)], we can exclude that it corresponds to a missing

TABLE II. Comparison of the unit cell parameters (a_1, a_2, θ) for both paired and compact layers on Cu(100) and on Cu(111). We have included the lattice parameters for the compact layer of Fc/Cu(111) [30].

Paired	a_1 (Å)	a_2 (Å)	θ (deg)
Nc/Cu(100)	12.6 ± 0.3	32.3 ± 0.8	41 ± 3
Nc/Cu(111)	12.9 ± 0.4	31.9 ± 0.4	42 ± 3
Compact			
Nc/Cu(100)	8.8 ± 0.4	15.1 ± 0.5	90 ± 2
Nc/Cu(111)	8.5 ± 0.4	15.7 ± 0.4	90 ± 3
Fc/Cu(111)	8.9 ± 0.3	15.5 ± 0.3	90 ± 3

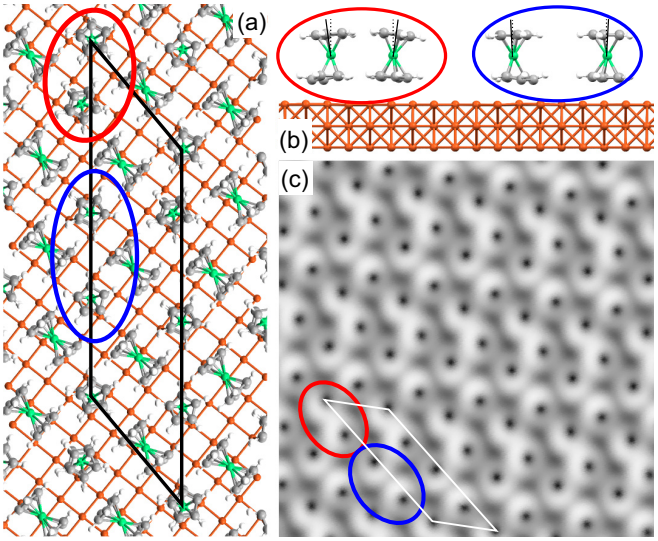

FIG. 6. (a) Top view of the optimized paired layer (only one layer of copper is represented), and (b) side view of the paired structure showing the tilt of the vertical molecules (horizontal molecules are omitted for clarity). The two type of Nc-Nc pairs are highlighted in blue and red, respectively. (c) Simulated STM image of the paired layer.

horizontal molecule, as artificially created vacancies with the STM tip resulted at least in corrugations higher than 1.5 Å (see Fig. S3 in the Supplemental Material). The exact nature of these defects is still unclear and will need further work to be determined.

In order to study the stability of the structures proposed for the molecular layer on Cu(100), we have performed extensive DFT+D2 calculations and simulated the corresponding STM images. While the carbon-surface distance for Nc is shorter than for Fc, the compact structure is strictly analogous to the one we previously proposed for ferrocene on Cu(111) [30] (see Fig. S1 and Table S2 in the Supplemental Material). Concerning the paired structure, we first justify the presence of horizontal molecules in addition to the vertical ones by performing atomistic calculations with [Fig. 6(a)] and without them. The adsorption energy is −1.52 eV in both cases and close to the one found for the compact layer (Table S2), pointing to a weak chemisorption as previously found for the isolated molecules. We remark, however, that without the horizontal molecules, only 15% of the adsorption energy comes from the nearest neighbors, increasing instead to 50% when the horizontal molecules are present. This shows that the surface-molecule interaction is weakened in the layer but compensated by interactions with the adjacent nickelocene molecules. The presence of horizontal molecules is, moreover, necessary to closely reproduce the structural features extracted from the experimental images. Horizontal molecules introduce a geometrical constraint causing the vertical molecules to tilt by 3° in the Nc-Nc pair with smallest spacing [the red circle in Fig. 6(b)] and by 8° in the other pair [the blue circle in Fig. 6(b)]. The vertical Nc are pushed up and stabilize at a position 0.1 Å higher than the one calculated for an isolated Nc (Table I), confirming the above energetic analysis of a weakened surface-molecule interaction. The simulated STM image [Fig. 6(c)] nicely matches the experimental one, contrary to the simulated image without horizontal molecules (see Fig. S2 in the Supplemental Material): The horizontal molecules cannot be seen and a corrugation of 0.8 Å is observed because of the tilt of the vertical molecules; the apparent height of the vertical Nc molecules is 0.4 Å higher compared to isolated Nc, in agreement with the findings of Fig. 2(d).

IV. CONCLUSION

To summarize, we have presented an experimental and theoretical study demonstrating that the chemical and electronic structure of nickelocene are preserved upon the adsorption on a noble metal surface such as copper. At low molecular coverages, nickelocene adsorbs vertically and is moderately chemisorbed. At higher coverages, Nc molecules self-assemble in two different layers, paired and compact, which are equally distributed across the surface. The layers, which include the presence of vertical and horizontal molecules, are stabilized by intermolecular vdW interactions. The T-shaped stacking geometry observed within these layers agrees remarkably with earlier findings on ferrocene [30] and therefore appears to be a general feature of metallocenes on metals. Future work will be devoted at tailoring the electronic and magnetic properties of Nc molecules through the on-surface metalation [39] or spin doping [12] of these layers.

ACKNOWLEDGMENTS

We gratefully thank N. Lorente for fruitful discussions. M.N.F. gratefully acknowledges J. Klimes for his advice. This work has been supported by the Agence Nationale de la Recherche (Grant No. ANR-13-BS10-0016). L.L. acknowledges financial support from the Agence Nationale de la Recherche through projects LabEx NIE (Grant No. ANR-11-LABX-0058 NIE) and LabEx CSC (Grant No. ANR-10-LABX-0026 CSC). We thank the national computational center IDRIS, CINES, and TGCC (Grant No. 2015-[x2015087364]) and the Lyon mesocenter PSMN for CPU time.

[1] S. Sanvito, Chem. Soc. Rev. **40**, 3336 (2011).
[2] A. Zhao, Q. Li, L. Chen, H. Xiang, W. Wang, S. Pan, B. Wang, X. Xiao, J. Yang, J. G. Hou, and Q. Zhu, Science **309**, 1542 (2005).
[3] L. Gao, W. Ji, Y. B. Hu, Z. H. Cheng, Z. T. Deng, Q. Liu, N. Jiang, X. Lin, W. Guo, S. X. Du, W. A. Hofer, X. C. Xie, and H.-J. Gao, Phys. Rev. Lett. **99**, 106402 (2007).
[4] J. J. Parks, A. R. Champagne, T. A. Costi, W. W. Shum, A. N. Pasupathy, E. Neuscamman, S. Flores-Torres, P. S. Cornaglia, A. A. Aligia, C. A. Balseiro, G. K.-L. Chan, H. D. Abruña, and D. C. Ralph, Science **328**, 1370 (2010).
[5] T. Komeda, H. Isshiki, J. Liu, Y.-F. Zhang, N. Lorente, K. Katoh, B. K. Breedlove, and M. Yamashita, Nat. Commun. **2**, 217 (2011).

[6] T. G. Gopakumar, F. Matino, H. Naggert, A. Bannwarth, F. Tuczek, and R. Berndt, Angew. Chem., Int. Ed. **51**, 6262 (2012).
[7] T. Miyamachi, M. Gruber, V. Davesne, M. Bowen, S. Boukari, L. Joly, F. Scheurer, G. Rogez, T. K. Yamada, P. Ohresser, E. Beaurepaire, and W. Wulfhekel, Nat. Commun. **3**, 938 (2012).
[8] B. W. Heinrich, G. Ahmadi, V. L. Müller, L. Braun, J. I. Pascual, and K. J. Franke, Nano Lett. **13**, 4840 (2013).
[9] R. Robles, N. Lorente, H. Isshiki, J. Liu, K. Katoh, B. K. Breedlove, M. Yamashita, and T. Komeda, Nano Lett. **12**, 3609 (2012).
[10] C. Krull, R. Robles, A. Mugarza, and P. Gambardella, Nat. Mater. **12**, 337 (2013)
[11] S. Stepanow, A. L. Rizzini, C. Krull, J. Kavich, J. C. Cezar, F. Yakhou-Harris, P. M. Sheverdyaeva, P. Moras, C. Carbone, G. Ceballos, A. Mugarza, and P. Gambardella, J. Am. Chem. Soc. **136**, 5451 (2014).
[12] M. Ormaza, R. Robles, N. Bachellier, P. Abufager, N. Lorente, and L. Limot, Nano Lett. **16**, 588 (2016).
[13] M. Urdampilleta, S. Klyatskaya, J.-P. Cleuziou, M. Ruben, and W. Wernsdorfer, Nat. Mater. **10**, 502 (2011).
[14] L.-J. Li, A. N. Khlobystov, J. G. Wiltshire, G. A. D. Briggs, and R. J. Nicholas, Nat. Mater. **4**, 481 (2005).
[15] V. M. García-Suáez, J. Ferrer, and C. J. Lambert, Phys. Rev. Lett. **96**, 106804 (2006).
[16] L. Zhou, S.-W. Yang, M.-F. Ng, M. B. Sullivan, Vincent B.C., and L. Shen, J. Am. Chem. Soc. **130**, 4023 (2008).
[17] L. Wang, Z. Cai, J. Wang, J. Lu, G. Luo, L. Lai, J. Zhou, R. Qin, Z. Gao, D. Yu, G. Li, W. N. Mei, and S. Sanvito, Nano Lett. **8**, 3640 (2008).
[18] R. Liu, S.-H. Ke, H. U. Baranger, and W. Yang, Nano Lett. **5**, 1959 (2005).
[19] Z. Yi, X. Shen, L. Sun, Z. Shen, S. Hou, and S. Sanvito, ACS Nano **4**, 2274 (2010).
[20] P. Abufager, R. Robles, and N. Lorente, J. Phys. Chem. C **119**, 12119 (2015).
[21] Z.-F. Xu, Y. Xie, W.-L. Feng, and H. F. Schaefer, III, J. Phys. Chem. A **107**, 2716 (2003).
[22] D. Welipitiya, C. Borca, C. Waldfried, C. Hutchings, L. Sage, C. Woodbridge, and P. Dowben, Surf. Sci. **393**, 34 (1997).
[23] D. Welipitiya, C. Waldfried, C. Borca, P. Dowben, N. Boag, H. Jiang, I. Gobulukoglu, and B. Robertson, Surf. Sci. **418**, 466 (1998).
[24] D. L. Pugmire, C. M. Woodbridge, S. Root, and M. A. Langell, J. Vac. Sci. Technol. A **17**, 1581 (1999).
[25] C. N. Borca, D. Welipitiya, P. A. Dowben, and N. M. Boag, J. Phys. Chem. B **104**, 1047 (2000).
[26] D. Pugmire, C. Woodbridge, N. Boag, and M. Langell, Surf. Sci. **472**, 155 (2001).
[27] Y. Li, X. Chen, G. Zhou, W. Duan, Y. Kim, M. Kim, and J. Ihm, Phys. Rev. B **83**, 195443 (2011).
[28] S. Marocchi, P. Ferriani, N. M. Caffrey, F. Manghi, S. Heinze, and V. Bellini, Phys. Rev. B **88**, 144407 (2013).
[29] See Supplemental Material at http://link.aps.org/supplemental/10.1103/PhysRevB.93.195403 for additional STM and DFT results, as well as details concerning the methods employed.
[30] M. Ormaza, P. Abufager, N. Bachellier, R. Robles, M. Verot, T. Le Bahers, M.-L. Bocquet, N. Lorente, and L. Limot, J. Phys. Chem. Lett. **6**, 395 (2015).
[31] J. A. Stroscio and R. J. Celotta, Science **306**, 242 (2004).
[32] B. W. Heinrich, C. Iacovita, T. Brumme, D.-J. Choi, L. Limot, M. V. Rastei, W. A. Hofer, J. Kortus, and J.-P. Bucher, J. Phys. Chem. Lett. **1**, 1517 (2010).
[33] J. Klimes, D. R. Bowler, and A. Michaelides, J. Phys.: Condens. Matter **22**, 022201 (2010).
[34] R. F. W. Bader, *Atoms in Molecules: A Quantum Theory* (Oxford University Press, Oxford, UK, 1990).
[35] R. F. W. Bader, P. L. A. Popelier, and T. A. Kleith, Angew. Chem., Int. Ed. **33**, 620 (1994).
[36] L. Hedberg and K. Hedberg, J. Chem. Phys. **53**, 1228 (1970).
[37] D. Zhong, K. Wedeking, T. Blömker, G. Erker, H. Fuchs, and L. Chi, ACS Nano **4**, 1997 (2010).
[38] N. A. Wasio, R. C. Quardokus, R. P. Forrest, C. S. Lent, S. A. Corcelli, J. A. Christie, K. W. Henderson, and S. A. Kandel, Nature (London) **507**, 86 (2014).
[39] B. W. Heinrich, L. Limot, M. V. Rastei, C. Iacovita, J. P. Bucher, D. M. Djimbi, C. Massobrio, and M. Boero, Phys. Rev. Lett. **107**, 216801 (2011).